

Tailoring conductive filaments by electroforming polarity in memristive based TiO₂ junctions

N. Ghenzi, M. J. Sánchez, D. Rubi, M. J. Rozenberg, C. Urdaniz, M. Weissman, and P. Levy

Citation: *Applied Physics Letters* **104**, 183505 (2014); doi: 10.1063/1.4875559

View online: <http://dx.doi.org/10.1063/1.4875559>

View Table of Contents: <http://scitation.aip.org/content/aip/journal/apl/104/18?ver=pdfcov>

Published by the *AIP Publishing*

Articles you may be interested in

[Impact of Joule heating on the microstructure of nanoscale TiO₂ resistive switching devices](#)

J. Appl. Phys. **113**, 163703 (2013); 10.1063/1.4803033

[Control of conducting filaments in TiO₂ films by a thin interfacial conducting oxide layer at the cathode](#)

Appl. Phys. Lett. **102**, 082903 (2013); 10.1063/1.4793577

[Transient characterization of the electroforming process in TiO₂ based resistive switching devices](#)

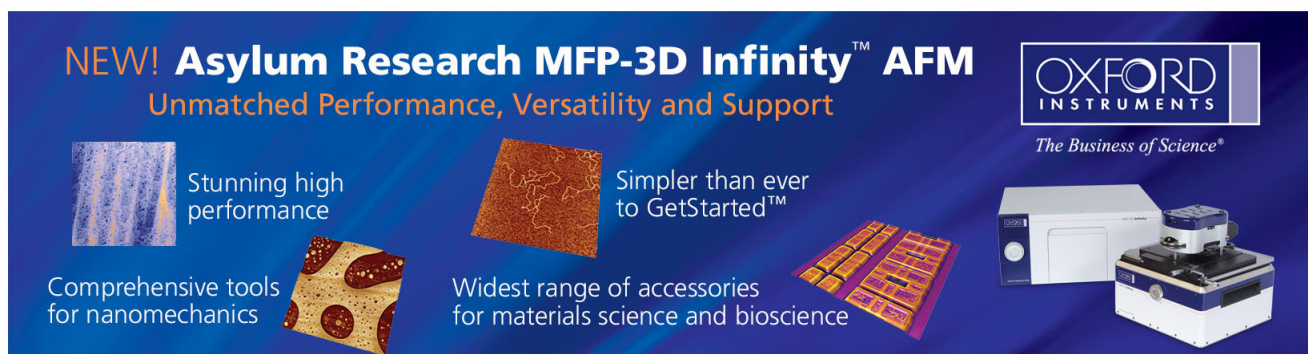
Appl. Phys. Lett. **102**, 023507 (2013); 10.1063/1.4776693

[Conducting nanofilaments formed by oxygen vacancy migration in Ti/TiO₂/TiN/MgO memristive device](#)

J. Appl. Phys. **110**, 104511 (2011); 10.1063/1.3662922

[Investigation statistics of bipolar multilevel memristive mechanism and characterizations in a thin FeOx transition layer of TiN/SiO₂/FeOx/Fe structure](#)

J. Appl. Phys. **110**, 053703 (2011); 10.1063/1.3630119

The advertisement features a dark blue background with white and orange text. At the top left, it reads 'NEW! Asylum Research MFP-3D Infinity™ AFM' in large white letters, followed by 'Unmatched Performance, Versatility and Support' in orange. On the right, the Oxford Instruments logo is shown with the tagline 'The Business of Science®'. Below the text are four images: a blue textured surface, a brown textured surface, a grid of colorful squares, and a photograph of the AFM instrument. Text descriptions are placed around these images: 'Stunning high performance' (top left), 'Simpler than ever to GetStarted™' (top right), 'Comprehensive tools for nanomechanics' (bottom left), and 'Widest range of accessories for materials science and bioscience' (bottom right).

Tailoring conductive filaments by electroforming polarity in memristive based TiO_2 junctions

N. Ghenzi,¹ M. J. Sánchez,^{2,3} D. Rubi,^{1,3,4} M. J. Rozenberg,^{3,5,6} C. Urdaniz,¹ M. Weissman,^{1,3} and P. Levy^{1,3}

¹GAIANN, Centro Atómico Constituyentes, Comisión Nacional de Energía Atómica, Buenos Aires, Argentina

²Centro Atómico Bariloche and Instituto Balseiro, CNEA, Río Negro, Argentina

³Consejo Nacional de Investigaciones Científicas y Técnicas (CONICET), Buenos Aires, Argentina

⁴ECyT, UNSAM, Martín de Irigoyen 3100, 1650 San Martín, Buenos Aires, Argentina

⁵Laboratoire de Physique des Solides, UMR8502 Université Paris-Sud, Orsay 91405, France

⁶Departamento de Física Juan José Giambiagi, FCEN, UBA, Buenos Aires, Argentina

(Received 8 February 2014; accepted 27 April 2014; published online 6 May 2014)

We probe the resistive switching response of Au/ TiO_2 /Cu junctions, on samples initialized using both polarities electroforming. A conductive path is formed in both cases: a copper metallic filament for negative electroforming and a titanium dioxide possibly Magnéli phase based filament for the positive case. We measured the resistance response of formed samples and studied their remanent resistance states. Bi (tri) stable resistance states were obtained for negative (positive) electroformed samples. The temperature dependence of the resistance discloses the underlying different nature of the associated filaments. In addition, we performed *ab initio* calculations to estimate the observed electroforming threshold voltages. © 2014 AIP Publishing LLC. [<http://dx.doi.org/10.1063/1.4875559>]

A reversible and non volatile change between two stable electric resistance states after the application of a pulsed electric stimulus (voltage or current) is observed in a variety of metal–oxide interfaces. Intense basic research^{1–4} focuses on this electric pulse induced Resistance Switching (RS) effect due to its potential use for the next generation of memory devices as it exhibits high retentivity time, multilevel states, reversibility, reliability, and low power consumption.^{5,6} The polarity dependent RS is called bipolar switching (BRS) and the polarity independent unipolar switching (URS). In BRS, the resistance change from high resistance state (HRS) to low resistance state (LRS)—set process—occurs at a certain voltage polarity, while the inverse reset process—from LRS to HRS—occurs at reversed voltage polarity. In principle, each type of switching requires quite different device specifications and operation ranges. Though it was recently reported that binary oxides based devices may exhibit both polarities RS and even coexistence.^{7–11} It is however still a challenge to correlate the experimental parameters with the sign of the forming polarity.

A crucial step in this direction is the electroforming process, which dictates the subsequent response in the device. Pristine samples display very high resistance (i.e., in the $G\Omega$ range), so the electrical initialization is necessary for RS to be observed.

The aim of this work is to analyze differences on the transport properties in Au/ TiO_2 /Cu asymmetric RS junctions, regarding the polarity of the initialization or forming process. We explore electroforming with both negative (F[−]) and positive (F⁺) polarities. Although we obtain reversible RS with linear LRS response for both forming polarities, the underlying mechanisms are found to be different. As we shall show, conducting filaments formed by different ionic species, either oxygen vacancies (OVs) or copper interstitials, can be generated depending on the forming polarity.

Based on our experiments and numerical calculations, we propose in both cases a possible RS mechanism.

We studied perpendicular Au (50 nm)/ TiO_2 (100 nm)/Cu (70 nm) junctions with electrode area of $20\ \mu\text{m} \times 20\ \mu\text{m}$ in a crossbar pattern (see inset of Fig. 1). Amorphous TiO_2 films were deposited by reactive sputtering with a pressure of 2.7 Pa, and a power of 150 W at room temperature. Bottom and top electrodes (BE and TE) were deposited by the thermal evaporation method and a lift-off process.¹³

Devices from the same crossbar pattern were initialized with either positive or negative voltage ramps. The electrical characterization was performed using a source–measurement unit Keithley 2612A, a personal computer with general purpose interface bus connections and Labview based software. Voltage pulses of variable amplitude and 1 ms time width were injected through the TE (with a delay of 100 ms

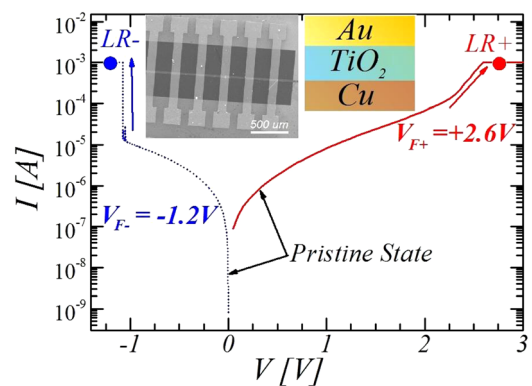


FIG. 1. Electroforming of Au (50 nm)/ TiO_2 (100 nm)/Cu(70 nm) junctions with negative (blue dotted line) and positive (red solid line) forming polarities. Note the two different forming voltages for F⁺ and F[−], respectively. After the electroforming, the sample is in the LR[−](LR⁺) for F[−](F⁺). Inset: SEM top view and schematic cross section of the TE(Au)/ TiO_2 /BE(Cu) structures. Devices are determined by the cross-link of a TE and a BE.

between pulses), while the BE was grounded. Between voltage pulses we read the remanent resistance using a small constant voltage of 0.1 V (Hysteresis Switching Loop curve, HSL). Thus, both dynamic (I-V curve) and remanent features are measured on the same run. Stable RS response was obtained after the initial electroforming procedure (see details below). For the formed junction, the RS properties (both I-V and HSL with alternating measurements) are recorded by applying a voltage ramp that started towards the opposite voltage polarity used in the electroforming, i.e., after positive (negative) electroforming, F+ (F-), the voltage ramp started towards negative (positive) voltages. The temperature dependence of the resistance was tested in a Liquid Nitrogen home made cryostat.

We start by describing the forming step for the F- case. By gradually increasing the voltage amplitude from 0 V to negative values, a sudden jump in the current was observed for $V_{F-} = -1.2$ V, as shown in Fig. 1 (blue dotted line). A current compliance I_{cc} of 1 mA was used to limit the abrupt flow of current. After this process, the device is in the LR state corresponding to the negative electroforming, labeled LR-.

Once the sample is formed, we analyzed the effect of further applying a triangular ramp between 0 and ± 1.3 V, starting towards positive values (see Fig. 2(a)). No current compliance was used in the positive branch, while in the negative one, I_{cc} was kept in a level of 5 mA to prevent permanent hard dielectric breakdown of the device. The LR- state exhibits a linear I-V dependence for positive stimulus as shown in Fig. 2(a). The reset process (i.e., the transition from LR- to HR-) is produced around +0.75 V at a current value of 6 mA. No additional transitions are observed up to +1.3 V. After reversing the voltage polarity, a set process is observed around -1.1 V, limited by $I_{cc} = 5$ mA. The described features, i.e., steep set/reset processes at different polarities and linear I-V dependence in the LR state are analogous to a fuse-antifuse polarity dependent switching mechanism.⁴

The HSL curve of the F- sample provides additional information on the remanent states. As observed in Fig. 2(b), the remanent resistance exhibits two well defined states around 100 Ω and 5 k Ω , namely, the LR- and HR- states, and two rapid transitions between them. A certain threshold voltage of positive pulsing stimulus (+0.75 V) is required to initiate the rapid upward change in the resistance from the LR- to the HR-. The total RS produces a ratio HR-/LR- \approx 50.

In the F+ case, the forming voltage is $V_{F+} = +2.6$ V (see Fig. 1, red solid line). It is meaningful to note the greater

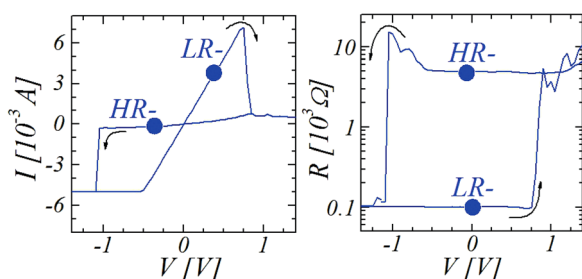


FIG. 2. (a) I-V and (b) HSL curves for negative electroformed samples, F-. The two stable states, LR- and HR-, are marked with circles.

amplitude and broader overall behaviour in the F+ case, as compared to the F-.

Figs. 3(a) and 3(b) show the I-V and HSL measurements after the F+ procedure, respectively. Current compliance was kept in a level of 2 mA for set/reset processes. After F+ the system is in a LR+ state, as shown in the HSL curve. In this curve, a sudden rise in the resistance is observed for small negative voltage just at the beginning of the loop cycle, reaching the HR+ state. Further increasing negative voltage renders a partial decrease in the resistance producing an “unexpected” set process to an intermediate resistance state, labeled IR+. When the voltage is turned to positive polarity again, the set process is produced to reach the initial LR+ state. This latter set process is the “standard” one, as it has the same voltage polarity of the forming F+. However, the partial set observed at negative voltage is “anomalous.” The obtained IR+ state develops around -0.4 V and is concomitantly depicted in the I-V curve at the “N shaped” region.

The I-V curve below ± 0.25 V in the F+ case is in qualitative agreement with previously reported data for TiO based memristive devices.³ Following the classification by Yang *et al.*,⁴ a continuous switching with origin symmetric features seems to be the case. In accordance, notice that the set transition has the same voltage amplitude than the reset transition, around ± 0.25 V.

The complete shape of the HSL protocol might resemble the “table with legs” characteristics observed in the HSL of manganites-based symmetric devices.¹⁴⁻¹⁶ However, in the last case, the presence of dips in the HSL curve was explained by the alternating activation of resistive switching in each one of the two metal-oxide interfaces, according to voltage polarity (BRS mode).^{17,18} In contrast, the interfacial mechanism² seems to be not appropriate to describe our experiments. The linear response of both LR states (LR- and LR+) in the I-V supports the absence of any constriction (to provide the interfacial behavior) or depinning energy related to Cu ions or OVs movement in the bipolar mode.¹⁹

A schematic representation of the proposed RS picture in the framework of filamentary conduction is presented in Fig. 4. The F- process driving the device to the LR- state, could in principle be explained as due to the formation of a filament composed of either OVs (Fig. 4(i)) or copper ions (Fig. 4(ii)). As the TE is negative biased, Cu+ could be attracted towards the Au electrode via migration through the TiO₂ film, acting like a solid electrolyte with soluble active electrodes (Ag and Cu) but not with noble metals.²⁰⁻²² It is also plausible that a filament composed of a Magneli or non

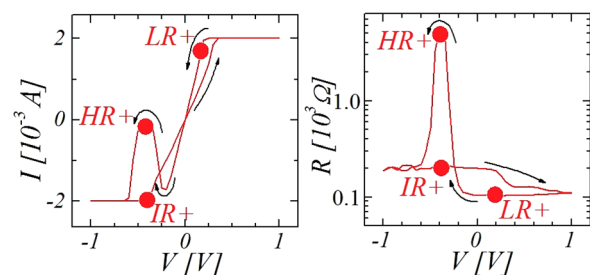


FIG. 3. (a) I-V curve and (b) HSL for the positive F+ formed device. The three stable states in the HSL, LR+, IR+, and HR+, are marked with circles.

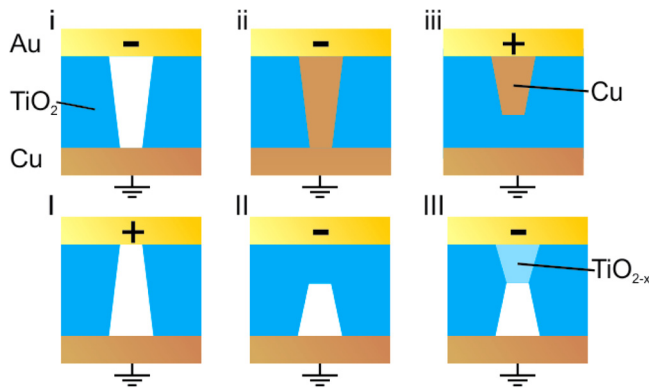


FIG. 4. Top row: Negative electroforming, F⁻: Sketch of filament composed either of (i) oxygen vacancy or (ii) by copper ions. (iii) The reset process breaks the copper filament in the thinnest part. Bottom row: Positive electroforming, F⁺: (I) Sketch of filament composed of OV. (II) The reset process breaks the OV filament due to re-oxidation of Ti. (III) A TiO_{2-x} region in series with the previous conductive filament is generated.

stoichiometric phase could produce the same behavior, as OV are positive defects too.²⁶ In both cases, the two stable (LR⁻ and HR⁻) resistance states could be obtained through a formation-rupture of the conductive filament.⁴ As we will demonstrate below, the formed filament in the case of the F⁻ process is actually associated to Cu drift. We shall come to this point later.

We now turn to the description of the F⁺ case. It is clear that Cu⁺ cannot drift from the BE, due to the direction of the electrical field. In this case, the LR⁺ state can be originated by the formation of a filament bridging the TE–BE composed of OV—due to the migration of oxygen ions from the BE to the TE—(see Fig. 4, bottom row I). To account for the tri-states observed in the F⁺ case, it is necessary to consider that, after the initial formation of the OV based filament, a reset process is produced for *negative* polarity. This process could be driven by the sudden re-oxidation of Ti probably attributed to oxygen vacancy annihilation at the Au/TiO₂ interface. This type of oxidation process has been widely reported previously for binary oxides with conductive filaments.^{27–29} It leads to a sudden break - up of the filament and the concomitant quick increase of the resistance (HR⁺ state, see Fig. 4, bottom row II). When the negative voltage is further raised, the transition from the HR⁺ state to the IR⁺ state follows. Notice that it occurs at a (negative) voltage which is smaller than the voltage of the LR⁻ transition. The reason is simply that this is an electric field driven transition and much of the TiO₂ is partially shorted by the broken low-resistance OV-filament. Thus, there is a large voltage drop, i.e., electric field, between the top electrode and the end of the broken filament. Within this high field a TiO_{2-x} region is promoted, filling the partially disrupted OV filament (see Fig. 4(III)), i.e., producing the IR⁺ state. Note that the weakest portion of this “composite filament” would be located deep inside the insulating matrix and not near to the electrodes, displaying an hourglass-like shape.¹²

Similar shaped conductive filaments were reported in Ref. 23. In addition other scenarios like hybrid filaments of copper interstitials and oxygen vacancies could be also possible and have been discussed in Refs. 24 and 25. When a positive stimulus is further applied the transition from IR⁺

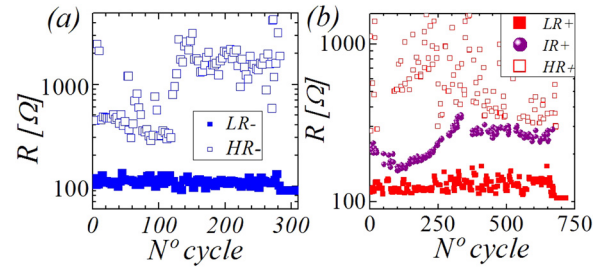


FIG. 5. Endurance characteristics of (a) F⁻ and (b) F⁺ electroformed samples. Triangular voltage ramps between ± 2 V have been applied. Devices are considered “exhausted” when they do not switch any more. In this case, the maximum number of cycles was 300 and 750 for F⁻ and F⁺, respectively.

to LR⁺ is attained. This is a relatively smaller effect (the resistance drops by just a factor of 2) and could be associated to a minor filament strengthening due to redistribution of mobile species.

The proposed description, though simple, results fully consistent with the whole experimental behaviour observed for the F⁺ sample. In addition, if the weakest switching region is effectively located deep into the oxide film, the efficiency of the Joule heating during the reset process should be maximized,¹² probably increasing the device endurance as compared to the F⁻ case.¹² We confirmed this hypothesis, by checking the endurance characteristics of both electroformed devices. As shown in Figs. 5(a) and 5(b), the positive electroformed device F⁺ exhibits the double # of cycles as compared to the negative electroformed device F⁻, before the full failure of the device.

In order to test the proposed nature of the involved filaments in both types of formed samples, we next focus on the study of both LR⁺ and LR⁻ resistance states, by decreasing temperature from room temperature to 90 K.

For the LR⁻, the obtained dependence exhibits a clear metallic behavior (see in Fig. 6 the line labeled by F⁻) consistent with the formation of a conductive filament originated by the diffusion of copper ions through the insulating matrix, introducing copper as interstitials. Denoting R_o the value of the LR⁻ resistance at room temperature, a positive temperature coefficient $\Delta R/(R_o \Delta T) = 0.0022 \text{ K}^{-1}$ is obtained from the experimental curve, in reasonable agreement with the reported value for bulk copper (0.0039 K^{-1}).

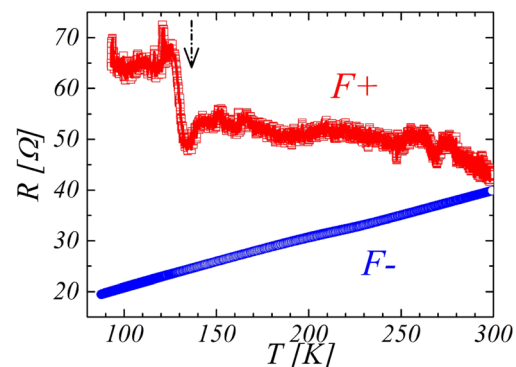


FIG. 6. Temperature dependence of the two low resistance states: for the F⁻ case, the LR⁻ is consisting with a copper filament connecting both electrodes and shows a metallic behaviour. In the F⁺ case, the LR⁺ is consistent with a Magneli phase based filament, showing a steep transition at 130 K.

On the other hand, the behavior of LR+ results consistent with a possible Magneli's phase based filament, with a low temperature coefficient. At 130K, the LR+ exhibits a sharp temperature induced transition, in agreement with previous reports.²⁶

Thus, the temperature dependence of the resistance discloses the underlying defects involved in each electroforming case, being copper ions and oxygen vacancies for the F− and F+ cases, respectively.

To estimate theoretically the relative probability of both conductive filaments, we performed *ab initio* calculations of the energy barriers for the drift of Cu+ interstitial ions and of neutral OV, along the (001) direction of rutile TiO₂. The calculations were based on density functional theory using the full potential Wien2k code³⁰ with the parameters given in Ref. 31 (see supplementary material for details³²).

We calculated the total energy of the TiO₂ supercell with an interstitial Cu+ ion in its more stable position and at the top of the barrier along the (001) direction. The energy difference between these two relaxed positions of Cu+ is 0.1 eV. For the diffusion of OV along (001), the energy difference between the vacancy located at an oxygen atom position or when the oxygen is at the midpoint between two planes along (001) is 0.9 eV after relaxation.^{33,34} This large difference in the energy required to move the two kinds of defects could be related to the fact that the forming voltage in the positive electroforming case F+ is higher than the forming voltage in the negative one F− and therefore in qualitative agreement with the results shown in Figure 1.

In summary, we studied the polarity dependent resistive switching characteristics of asymmetric Au/TiO₂/Cu junctions exhibiting memristive properties. We considered both polarities electroforming and studied their electrical features (both dynamical and remanent response to voltage pulses) and their temperature dependence. We showed the determinant role of the electroforming polarity on TiO₂ based memory devices, which produces the migration of either Cu or OV to develop conducting filaments. Besides, a device with three stable states (LR+, IR, and HR+) was obtained after a single electroforming procedure.

We obtained support from PIP 20080047 “MeMo”, “MeMOSat” Project and PIP11220080101821. D.R. acknowledges financial support from CONICET (PIP 291).

¹G. I. Meijer, *Science* **319**, 1625 (2008).

²A. Sawa, *Mater. Today* **11**, 28 (2008).

³R. Waser, R. Dittmann, G. Staikov, and K. Szot, *Adv. Mater.* **21**, 2632 (2009).

⁴J. J. Yang, I. H. Inoue, T. Mikolajick, and C. S. Hwang, *MRS Bull.* **37**, 131 (2012).

- ⁵C. Nauenheim, in *8th IEEE Conference on Nanotechnology (NANO'08)* (2008), Vol. 464, pp. 534–537.
- ⁶J. J. Yang, D. B. Strukov, and D. R. Stewart, *Nat. Nanotechnol.* **8**, 13 (2013).
- ⁷D. S. Jeong, H. Schroeder, and R. Waser, *Electrochem. Solid State Lett.* **10**, G51–G53 (2007).
- ⁸D. S. Jeong, H. Schroeder, and R. Waser, *Phys. Rev. B* **79**, 195317 (2009).
- ⁹N. Ghenzi, P. Stoliar, M. C. Fuertes, F. G. Marlasca, and P. Levy, *Physica B* **407**, 3096 (2012).
- ¹⁰I. Valov, R. Waser, J. R. Jameson, and M. N. Kozicki, *Nanotechnology* **22**, 254003 (2011).
- ¹¹T. Liu, M. Verma, Y. Kanga, and M. K. Orłowska, *ECS Trans.* **45**, 279 (2012).
- ¹²G. H. Kim, J. H. Lee, J. Y. Seok, S. J. Song, J. H. Yoon, K. J. Yoon, M. H. Lee, K. M. Kim, H. D. Lee, S. W. Ryu *et al.*, *Appl. Phys. Lett.* **98**, 262901 (2011).
- ¹³N. Ghenzi, D. Rubi, E. Mangano, G. Giménez, P. Stoliar, and P. Levy, *Thin Solid Films* **550**, 683 (2014).
- ¹⁴Y. B. Nian, J. Strozier, N. J. Wu, X. Chen, and A. Ignatiev, *Phys. Rev. Lett.* **98**, 146403 (2007).
- ¹⁵M. J. Rozenberg, M. J. Sánchez, R. Weht, C. Acha, F. Gomez-Marlasca, and P. Levy, *Phys. Rev. B* **81**, 115101 (2010).
- ¹⁶N. Ghenzi, M. J. Sánchez, F. G. Marlasca, P. Levy, and M. J. Rozenberg, *J. Appl. Phys.* **107**, 093719 (2010).
- ¹⁷F. G. Marlasca, N. Ghenzi, P. Stoliar, M. J. Sánchez, M. J. Rozenberg, A. G. Leyva, and P. Levy, *Appl. Phys. Lett.* **98**, 123502 (2011).
- ¹⁸N. Ghenzi, M. J. Sánchez, M. J. Rozenberg, P. Stoliar, F. G. Marlasca, D. Rubi, and P. Levy, *J. Appl. Phys.* **111**, 084512 (2012).
- ¹⁹N. Ghenzi, M. J. Sánchez, and P. Levy, *J. Phys. D: Appl. Phys.* **46**, 415101 (2013).
- ²⁰K. Tsunoda, Y. Fukuzumi, J. R. Jameson, Z. Wang, P. B. Griffin, and Y. Nishi, *Appl. Phys. Lett.* **90**, 113501 (2007).
- ²¹Y. Kang, M. Verma, T. Liu, and M. K. Orłowski, *ECS Solid State Lett.* **1**, Q48 (2012).
- ²²T. Nagata, M. Haemori, Y. Yamashita, H. Yoshikawa, Y. Iwashita, K. Kobayashi, and T. Chikyow, *Appl. Phys. Lett.* **99**, 223517 (2011).
- ²³K. J. Yoon, M. H. Lee, G. H. Kim, S. J. Song, J. Y. Seok, S. Han, J. H. Yoon, K. M. Kim, and C. S. Hwang, *Nanotechnology* **23**, 185202 (2012).
- ²⁴L. Yang, “Resistive switching in TiO₂ thin films,” Ph.D. thesis (JARA, Julich, Germany, 2010).
- ²⁵F. Yuan, J. Wang, Z. Zhang, Y. Ye, L. Pan, J. Xu, and C. S. Lai, *Appl. Phys. Express* **7**, 024204 (2014).
- ²⁶D. H. Kwon, K. M. Kim, J. H. Jang, J. M. Jeon, M. H. Lee, G. H. Kim, X. S. Li, G. S. Park, B. Lee, S. Han *et al.*, *Nat. Nanotechnol.* **5**, 148 (2010).
- ²⁷S. J. Song, J. Y. Seok, J. H. Yoon, K. M. Kim, G. H. Kim, M. H. Lee, and C. S. Hwang, *Sci. Rep.* **3**, 3443 (2013).
- ²⁸T. Yanagida, K. Nagashima, K. Oka, M. Kanai, A. Klamchuen, B. H. Park, and T. Kawai, *Sci. Rep.* **3**, 1657 (2013).
- ²⁹M. C. Urdaniz, M. A. Barral, and A. M. Llois, *Phys. Rev. B* **86**, 245416 (2012).
- ³⁰P. Blaha, *Wien2k, an Augmented Plane Wave Plus Local Orbitals Program for Calculating Crystal Properties*, edited by K. Schwarz (Technische Universität Wien, Austria, 2001).
- ³¹For the FP-LAPW calculations we used the GGA exchange and correlation potential, and parameters $R_{Kmax}=6$, 50 K points and muffin tin radii reduced so that they would not touch at the barrier top.
- ³²See supplementary material at <http://dx.doi.org/10.1063/1.4875559> for details of *ab initio* calculations.
- ³³H. Iddir, S. Ogut, P. Zapol, and N. Browning, *Phys. Rev. B* **75**, 073203 (2007).
- ³⁴M. Weissmann and R. Weht, *Phys. Rev. B* **84**, 144419 (2011).